The Interaction of CO and W(111) Surface

S. Y. Lee, Y. -D. Kim, S. N. Seo, C. Y. Park,† H. T. Kwak,‡ J. -H. Boo, and S. B. Lee*

Department of Chemistry, Sungkyunkwan University, Suwon 440-746, Korea
†Department of Physics, Sungkyunkwan University, Suwon 440-746, Korea
‡Department of Chemistry, Kook Min University, Seoul 136-701, Korea
Received February 2, 1999

The adsorption of CO on W(111) surface in the range of adsorption temperature between 300 K and 1000 K has been studied using AES, LEED, and TDS in an UHV system. After CO saturation at 300 K, four desorption peaks are observed at temperatures (K) of about 400, 850, 1000, and 1100 in thermal desorption spectra, called as α, β_1, β_2, and β_3 state, respectively. The state was attributed to molecular species of CO, which is well known. Because the CO in β states (especially the β_3 state) is still debated as to whether it is dissociative or non-dissociative, the β_3 state is mainly discussed. By using the variation method of heating rate in the thermal desorption spectrometry, the desorption energy and pre-exponential factor for the β_3 state are evaluated to be 280 kJ/mol and 1.5×10^{12} s^{-1}, respectively. A lateral interaction energy of 5.7 kJ/mol can also be estimated by Bragg-Williams approximation. To interpret the thermal desorption spectra for the β_3 state, moreover, those for the model of a first order and a second order desorption are simulated using quasi-chemical approximation. In this study, a model of lying-down CO species is proposed for the β_3 state of CO adsorption.

Introduction

Over the last 30 years, the interaction of carbon monoxide with tungsten has been extensively studied with a wide variety of techniques including low energy electron diffraction (LEED), photoelectron spectroscopy and thermal desorption spectroscopy (TDS), leading to the publication of several reviews.[1-5] Despite extensive studies of this system, a number of questions regarding structure and kinetics remain unresolved.

Thermal desorption spectra of CO desorbed from the tungsten surfaces have shown two main desorption states; one of them, called α, appears at about 400 K and the other, called β, shows two or three desorption peaks in the range of about 800 K to 1300 K, depending on surface conditions and surface plane. On W(100), for example, CO exhibits four major binding states, occurring at 400 K, 1000 K, 1100 K, and 1450 K, respectively. All of these obey the first order desorption kinetics except the most tightly bound state, which follows second order kinetics.[6,7] For W(110),[8,9] desorption spectra of two α states, one virgin state, and two β states, with the first order desorption kinetics, have been observed at 200-450 K for α and virgin states, 850-1000 K for β_1, and 975-1250 K for β_2. In the case of W(111), however, we found only two published papers[10-11] concerning the TDS study. But in each paper, only a single TD experiment was carried out using a CO saturated W(111) surface, suggesting inconclusive resu- lts. Regarding the α state, it has been believed that it is due to a molecular species of end-on type on the surface, based on the TDS experimental data, vibrational spectroscopy and photoelectron spectroscopy. On the other hand, the structure of the β state has always been subject to controversy.

Even up until early 1970, non-dissociative adsorption of CO was in general, accepted on the basis of the fact that no sign of carbon and oxygen on the surface is observed by field emission microscopy even after repeated adsorption/ desorption. Also, the diffusion of CO in β states does not occ- ur below 700 K, which is quite different from the fact that the adsorbed pure oxygen is mobile even below 400 K.[1] Moreover, the desorption of CO from the β state as well as α state follows the first order kinetics and only CO desorbing above about 850 K is isotopically mixed.[1] Goymour and King[12-14] observed, however, that desorption peaks for the β_2 appearing near 1500 K shifted to a lower temperature with increasing coverage, and they proposed a dissociative model. Acco- rding to this model, the CO in the β states is dissociated into W-C and W-O, and upon heating of the C and O atoms, recombine to desorb as CO. Experimental results obtained by photoelectron spectroscopy,[15-17] vibrational spectroscopy[18,19] and electron stimulated desorption[12,20,21] have been expla-ined on the basis of the dissociative model. It is now widely accepted that the adsorption of CO in β states is dissociative. Up to now, however, it has not been explained very well that, if it is possible to dissociate the CO at high temperature, why are not C or O atoms observed on tungsten surface after re- peated desorption, and why no diffusion of O atom formed by dissociation of CO occurs at high temperature in opposition to the dissociatively adsorbed O atoms from pure oxygen molecules.

According to our experimental data,[22] the binding energies of the O(1s) and C(1s) x-ray photoelectron peaks observed at 1000 K for β_3-CO do not coincide with that of O_2 adsorption. This indicates that oxygen species in the β_3 state are clearly different from the dissociative oxygen by O_2 adsorption. Moreover, UPS also shows that with the surface temperatures increasing from room temperature to 1100 K, peaks quite different from previous ones are observed at below Fermi energy of 6.5 eV and 7.1 eV. These peaks are clearly different from the O(2p) valence peak induced from dissociatively adsorbed oxygen atoms. This should received

special attention due to the inequality of the binding energy (B. E.) of O, which is in contrast to the equality of the B. E. of O(1s) between β_3 state and the dissociative oxygen of O_2 adsorption on the W(110) and (111) surfaces.

To confirm our XPS and UPS data more precisely, we report here the TDS results for the carbon monoxide on W (111) surface, which differs from the previous results observed for the tungsten surfaces with different Miller index planes.

Experimental Section

The experiments are performed in a conventional ultra high vacuum (UHV) chamber with a base pressure of 1×10^{-10} Torr. The chamber is equipped with a quadrupole mass spectrometer (QMS) for residual gas analysis and, for the thermal desorption spectroscopy (TDS), 4-Grid Optics for low energy electron diffraction (LEED). A concentric hemispherical analyzer (CHA) is also included for electron energy analysis. In addition, there are a grazing incidence electron gun for Auger electron spectroscopy (AES), He-discharge lamp for ultraviolet photoelectron spectroscopy (UPS), and dual anode x-ray source for x-ray photoelectron spectroscopy (XPS). More details of the system are found in the previous publication.[23]

The tungsten sample used in this experiment was oriented toward (111) direction within 0.5° of the (111) plane. It is a disk type approximately 1 cm in diameter and 1.5 mm in thickness. The crystal was spot-welded onto a pair of W wire (0.2 mm), which were themselves spot-welded onto a pair of parallel Mo rods (1.5 mm in diameter). The Mo rods were directly connected to a pair of Cu blocks, which were then connected to an electrical feedthrough to heat the crystal resistively. W-5% Re/W-26% Re thermocouple was spotwelded to the edge of the crystal for temperature measurement.

The sample was cleaned by exposing it at 1300 K under 10^{-8} Torr of O_2 followed by Ar-ion sputtering and annealing for 60s at 1400 K, repeatedly. Clean surface was confirmed by AES and LEED. The range of heating rates used for TDS experiments was 4 K/s to 10 K/s and the temperature was increased linearly to 1350 K.

Results and Discussion

Figure 1 shows thermal desorption spectra for CO adsorbed on W(111) with CO exposures at 300 K. This exhibits α state at 410 K and β states in the range of 800 K to 1200 K. The three peaks at 850 K, 1000 K, and 1150 K in states were distinguished, and we labeled these peaks as β_1, β_2, and β_3, respectively. The β_3 peak started to grow from low CO exposure and reached near saturation coverage after CO exposure of 1.5 L. The β_1 and β_2 peaks began to appear after 1.5 L CO exposure. But although the α state was observed even at low CO coverages, the peak increased markedly only after saturation of the β_3 state with increasing CO exposures. These spectra are similar with those obtained previously for W (111).[10,11]

Since the desorption kinetic order and the desorption temperature of α state agrees with the previous work of others,[2] we believe that the α state is due to a molecular species with an end-on configuration based on the data of photoelectron spectroscopy.[3,15,16] Many previous spectroscopic data have been interpreted in view of dissociation of CO for the β states. However, the desorption kinetic order and the shape of desorption spectra for the β_3 state in Figure 1 suggest non-dissociative adsorption of CO. Figure 2 shows a series of thermal desorption spectra for the β_3 state, which are easily separated from the other β states by adsorption of CO at 1000 K. Any significant difference in TD spectra between the β_3 state obtained for CO adsorption at 1000 K and that obtained for the CO adsorbed at 300 K and annealed at 1000 K was not found. These spectra show that the peak maxima shift to higher temperatures with increasing the CO exposure. This is significantly different from data obtained previously. As it is known generally, such a shift indicates attractive lateral interaction in the adsorbed layer. And the asymmetric shape of a tail in the low temperature side agrees well with that of the molecular desorption. This means that the β_3 state consists of non-dissociative species and that there is an attractive force between adsorbed species. Since CO possesses the highest chemical bond strength of any molecule, we can reject the dissociation hypothesis and employ a bimolecular isotope exchange model involving ''inclined'' CO molecules bound via both C and O atoms to the surface W atoms.

Assuming the first order desorption kinetics, the relationship between the temperature of peak maximum and the variation of heating rate is expressed from Redhead equation as follows,[24]

$$ln(T_p^2/\beta) = E_d/RT_p + ln(E_d/vR)$$

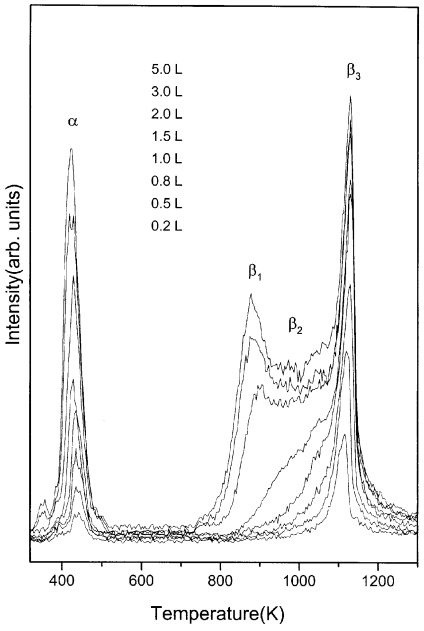

Figure 1. Thermal desorption spectra of CO adsorbed on W(111) with various CO exposures at 300 K.

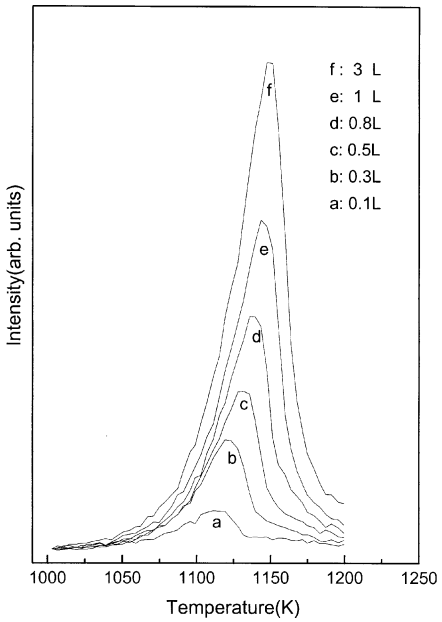

Figure 2. A series of thermal desorption spectra for β_3 state with various CO exposures.

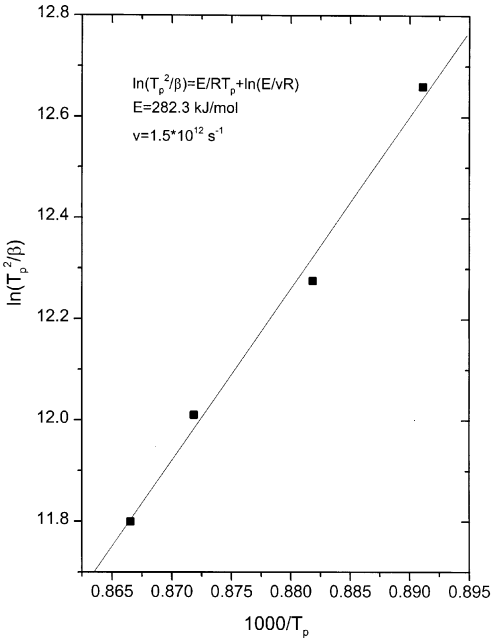

Figure 3. The plot of ln (T_p^2/β) to $1/T_p$.

where T_p is peak maximum temperature, β heating rate, E_d activation energy of desorption, and v pre-exponential factor. From the temperature maxima with variation of heating rate, the activation energy of desorption and pre-exponential factor can be determined. By taking the heating rate (K/s) of 4, 6, 8, and 10, thermal desorption spectra for 5 L CO exposure at 1000 K were recorded. From the shift of the maximum temperature of desorption spectra with the variation of heating rate, the plot of ln (T_p^2/β) to $1/T_p$ was shown in Figure 3. The desorption activation energy and the pre-exponential factor obtained from the slope and intercept of the plot are 280.3 kJ/mol and 1.5×10^{12} s^{-1}, respectively.

According to the Bragg-Williams approximation for a molecular desorption,[25] the desorption rate, r_d is written as follows,

$$r_d = -d\theta/dt = \nu\theta \exp[-(E_{0,d} - z\varepsilon_{AA}\theta)/kT]$$

where is coverage of adsorbed species, $E_{0,d}$ zero coverage desorption energy, z the number of the nearest adsorbed species around an adsorbed species, and ε_{AA} lateral interactions between the adsorbed species. When this equation is compared to Polanyi-Wigner equation for the first order desorption kinetics, the desorption activation energy is written as follows,

$$E_d = E_{0,d} - z\varepsilon_{AA}\theta$$

Lateral interaction energy can be estimated from the slope of the plot for the variation of desorption energy with coverage. Figure 4 shows desorption energies as a function of the CO coverage, which are calculated by Redhead equation from a series of thermal desorption spectra as shown in Figure 2. The initial desorption energy at $\theta = 0$ is evaluated to be 272 kJ/mol from the intercept. The number of nearest species, z, is taken to be 2, because the LEED pattern for β_3 state shows (7×1) structure and the amount of CO desorbed from

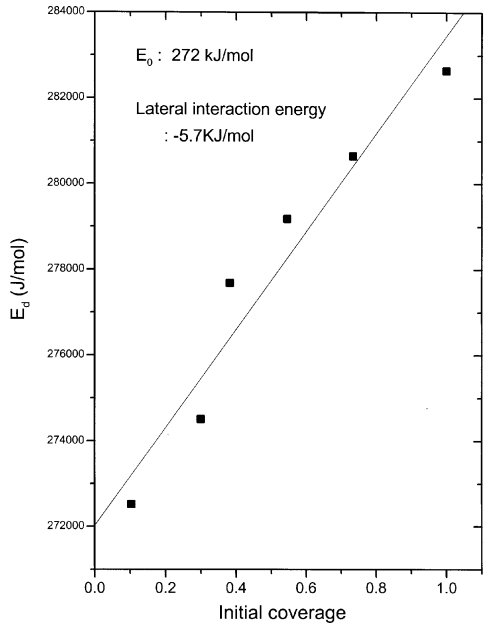

Figure 4. The desorption energies as a function of coverage.

the β_3 state is about 1/3 of the total amount of CO desorbed from W (111) surface. Based on the values for z and θ, the lateral interaction energy, $\varepsilon_{AA,}$ of –5.7 kJ/mol (negative for attraction) is estimated from the slope of the plotted line in Figure 4, and the desorption energy for full coverage of the β_3 state is evaluated to be 275.8 kJ/mol, a value close to that obtained by the variation of heating rate for the exposure of 5 L CO (280.3 kJ/mol).

To examine whether the adsorption of CO in β_3 state is associative or dissociative in detail, the thermal desorption spectra with increasing CO coverage were simulated for a first order desorption and a second order desorption by combination of two adatoms, using the following quasi-chemical approxima-

tion.[26,27]

For a first order desorption ($A_{(ad)} \rightarrow A(g)$),

$$r_d = \nu \exp(-E_d/kT)\theta f_d^{(1)}(\theta, \varepsilon_{AA})$$

where

$$f_d^{(1)}(\theta, \varepsilon_{AA}) = [\{P_{AA}\exp(\varepsilon_{AA}/kT) + 0.5P_{AO}\}/\theta]^z$$

For a second order desorption ($A_{(ad)}+A_{(ad)} \rightarrow A_2(g)$),

$$r_d = \nu \exp(-E_d/kT) f_d^{(2)}(\theta, \varepsilon_{AA})$$

where

$$f_d^{(2)}(\theta, \varepsilon_{AA}) = P_{AA}[\{P_{AA}\exp(\varepsilon_{AA}/kT) + 0.5P_{AO}\}/\theta]^{2z-2}$$

and ε_{AA} is related to lateral interactions between nearest-neighbor pairs of adsorbed molecules, P_{AA} is the probability that the nearest sites are occupied by the pair AA, and P_{AO} is the probability that one of the nearest sites is occupied by adsorbed species, and the other one remains vacant. The following parameters have been used in the calculations: $z = 2$ (linear structure assumed from the LEED pattern), $E_d = 272$ kJ/mol and $\nu = 1.5 \times 10^{12}$ s^{-1}. The simulated spectra is shown in Figure 5, where (a) is the first order desorption and (b) is the second order desorption by recombination of two adsorbed species. As shown in Figure 5(a), the peak maxima of simulated desorption spectra for the first order desorption shift monotonously to higher temperature with increasing CO coverage. On the other hand, the simulated spectra for the second order desorption model show that the maximum desorption temperatures decrease with increasing CO coverages, initially, and then increase slowly. The simulated spectra for the first order desorption are very similar to those obtained experimentally for β_3 state. This result strongly supports that CO in β_3 state on W(111) surface is non-dissociative species, that is, CO in β_3 state adsorbs molecularly rather than dissociatively.

Two types have been traditionally considered as a model of adsorbed molecular species of CO. One of them is an end-on species and the other is a lying-down species. Considering some attractive interaction between adsorbed species and a very high desorption energy of about 270 kJ/mol, the lying-down species represents more likely the β_3 state. This model agrees with the fact that no traces of carbon and oxygen were found on the surface after repeated cycles of adsorption and desorption in earlier works as well as in our experiments. Moreover, this lying-down model agrees well with the model of four-centered bimolecular complex with the lying-down species. Madey *et al.*[28] observed a fast isotope exchange reaction of CO on polycrystalline tungsten surface at above 850 K when the $C^{12}O^{18}$ and the $C^{13}O^{16}$ were coadsorbed molecularly. To explain the kinetics of this result, they suggest a four-centered bimolecular complex with lying-down configuration. With the lying-down model of CO, isotope exchanges of CO in β state and isotope substituted atomic oxygen on W(100), (110), and (111) surfaces found by Anders and Hansen[17] can also be explained by the following surface complex, although they have supported the dissociative chemisorption of CO without good evidence.

$$CO^{16}{}_{ad} + O^{18}{}_{ad} \rightarrow [O^{16}\text{-}C\text{-}O^{18}] \rightarrow CO^{16} \text{ or } CO^{18}$$

A molecular orbital calculation for interaction of CO on W (111) surface using the atom superposition and electron delocalization molecular orbital method[29] shows that the CO molecule in the lying-down configuration is the most stable due to the interaction of 5σ orbital in CO with sp-band in W surface. Similar results have been obtained by Mehandru and Anderson.[30] Their results also support the lying-down model proposed in this work. And the lying-down species is also supported by the XPS and UPS results performed in our

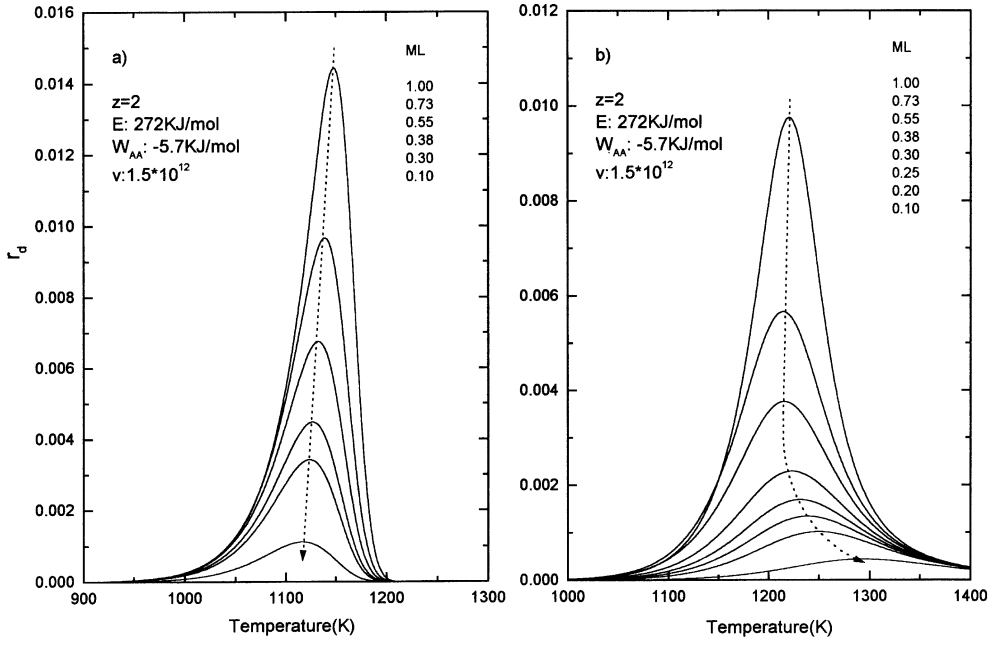

Figure 5. The simulated thermal desorption spectra by quasi-chemical approximation. a) first order desorption, b) second order desorption.

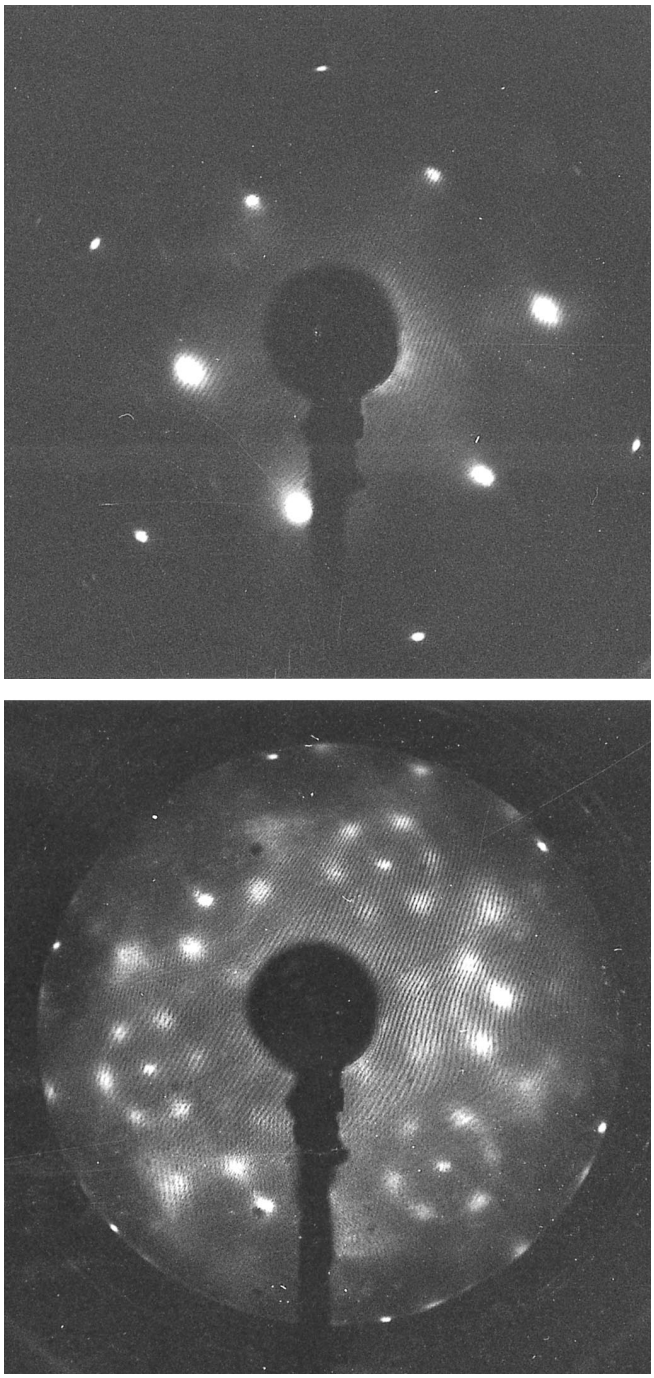

Figure 6. LEED patterns at 68.3 eV. (above) for clean surface of W(111), (bottom) for β_3 state.

laboratory.[31] These experimental results show that the electron binding energy of O(1s) and valence band of adsorbed CO in β_3 state differ from those of adsorbed atomic oxygen on W surface. These differences in binding energy are explained in view of non-dissociative adsorption of CO in β_3 state.

A superstructure was for the first time observed in the LEED pattern for adsorption of CO on W(111). Even though adsorption of CO on W(111) at room temperature did not reveal any new superstructures for all CO coverages, the original spots of hexagonal structure that represents (1×1) pattern for the clean W(111) surface showed increasing diffusion with increasing CO exposures. This means that carbon monoxide adsorbs irregularly on W(111) surface. But when the adsorbed layer formed under exposure of 5 L CO was heated to about 1000 K, a complex superstructure was observed in LEED pattern as shown in the bottom of Figure 6. This superstructure does not exhibit any difference in LEED pattern between that observed for CO adsorbed at 1000 K and that observed after heating the adsorbed CO at room temperature to 1000 K. Because the adsorption of 5 L CO at 1000 K represents the β_3 state in TDS, the superstructure corresponds to the β_3 state. Since no measurement of spot intensities with electron beam energies was performed, the CO adsorption geometry for the superstructure could not be determined here. However, the similar LEED pattern was observed by Van Hove et al. for adsorption of CO on Cu(111) surface.[32] They interpreted it as three equivalent rotated (7×1) structures having missing spots in the 1, 3, 4, 7 positions from (0,0) spot. Based on the (7×1) structure, the amount of adsorbed CO in β_3 state corresponds to about 30 percent of tungsten surface atoms (*i.e.* 5.1×10^{14} atoms/cm^2). This agrees well with the coverage of about 0.3 estimated from TDS.

Conclusions

The desorbed CO from the β_3 state follows the first order desorption kinetics. This implies that there is a lateral attraction between the adsorbed species. This results suggest a non-di- ssociative lying-down species of adsorbed CO in the β_3 state rather than the dissociative adsorption of CO. The detailed analysis of TDS supports the non-dissociative lying-down species. This is also consistent with our XPS and UPS res- ults.[25] As a result, the desorbed CO from β_3 state in the range of 800 K to 1200 K should be non-dissociative adsorbed CO.

Acknowledgment. This work was supported by the Basic Science Research Institute Program (BSRI-95-6401), Ministry of Education, Korea, and in part by the Korea Science and Engineering Foundation (Grant Nos. 95-0501-09 and 961-0305-045-1).

References

1. Ford, R. R. *Adv. Catal.* **1970**, *21*, 51.
2. King, D. A.; Goymour, C. G.; Yates, Jr., J. T. *Proc. Royal Soc.* (London) **1972**, *A331*, 361.
3. Plummer, E. W.; Waclawski, B. J.; Vorvurger, T. V.; Kuyatt, C. E. *Prog. Surf. Sci.* **1976**, *7*, 149.
4. Campuzano, J. C. In *The Chemical Physics of Solid Surfaces and Heterogeneous Catalysis*; King, D. A., Woodruff, D. P., Eds; Elsevier, Amsterdam; New York, 1990; part A, vol. 3, p 389.
5. Yates, Jr., J. T. *Surf. Sci.* **1994**, *299/300*, 731: see also Dong, C. Z.; Shivaprasad, S. M.; Song, K. J.; Madey, T. E. *J. Chem. Phys.* **1993**, *99*(11), 9172.
6. Clavenna, L. R.; L. D. Schmidt, L. R. *Surf. Sci.* **1972**, *33*,

11.
7. Wang, C.; Gomer, R. *Surf. Sci.* **1979**, *90*, 10.
8. Kohrt, C.; Gomer, R. *Surf. Sci*. **1971**, *24*, 77.
9. Kohrt, C.; Gomer, R. *J. Chem. Phys*. **1970**, *52*, 3283.
10. Anders, L. W.; Hansen, R. S. *J. Chem, Phys.* **1975**, *62*, 4652.
11. Dong, C. Z.; Zhang, L.; Diebold, U.; Madey, T. E. *Surf. Sci.* **1995**, *322*, 221.
12. Goymour, C. G.; King, D. A. *Chem. Soc. Faraday Trans.1*, **1973**, *69*, 736.
13. Goymour, C. G.; King, D. A. *Chem. Soc. Faraday Trans.1*, **1973**, *69*, 749
14. Goymour, C. G.; King, D. A. *Surf. Sci.* **1973**, *35*, 246.
15. Umbach, E.; Fuggle, J. C.; Menzel, D. *J. Electron Spec. and Rel. Phenom*. **1977**, *10*, 15.
16. Bradshaw, A. M.; Menzel, D.; Steinkilberg, M. *Chem. Phys. Letters* **1974**, *28*, 516.
17. Umbach, E.; Menzel, D. *Surf. Sci.* **1983**, *135*, 199.
18. Froitzheim, H.; Ibach, H: Lehwald, S. *Surf. Sci*. **1977**, *63*, 56.
19. Franchy, R.; Ibach, H. *Surf. Sci*. **1985**, *155*, 15.
20. Madey, T. E.; Czyzewski, J. J.; Yates, Jr., J. T. *Surf. Sci*. **1976**, *57*, 580.
21. Jaeger, R.; Menzel, D. *Surf. Sci*. **1980**, *93*, 71.
22. Lee, S.-B., In *Proc. of the Oji Seminar on chemical processes at surfaces based on atomic scale structure and dynamics*, Tanaka, K., Eds.; WORDS Publishing House: Tokyo, 1996; p 83.
23. Lee, S. B.; Kang, D. H.; Park, C. Y.; Kwak, H. T. *Bull. Korean Chem. Soc*. **1995**, *16*, 157.
24. Redhead, P. A. *Vacuum* **1962**, *12*, 203.
25. Bragg, W. L.; Williams, E. J. *Proc. Royal Soc.* (London) **1934**, *A145*, 699.
26. Zhdanov, V. P. *Surf. Sci*. **1981**, *111*, 63.
27. Zhdanov, V. P. *Surf. Sci*. **1983**, *133*, 469.
28. Madey, T. E.; Yates, Jr., J. T.; Stern, R. C. *J. Chem. Phys*. **1965**, *42*, 1372.
29. Ryu, G.; Park, S. C.; Lee, S. B. *Surf. Sci.* **1999**, *427/428*, 261.
30. Mehandru, S. P.; Anderson, A. B. *Surf. Sci.* **1988**, *201*, 345.
31. Lee, S. Y.; Kim, Y.-D.; Yang, T. S.; Park, C. Y.; Kwak, H. T.; Boo, J.-H.; Lee, S. B. in preparation.
32. Biberian, J. P.; Van Hove, M. A. *Surf. Sci*. **1984**, *138*, 361.